

Multi-Modal Diffusion for Hand-Object Grasp Generation

Jinkun Cao*¹ Jingyuan Liu² Kris Kitani¹ Yi Zhou²
¹ Carnegie Mellon University ²Adobe

Abstract

In this work, we focus on generating hand grasp over objects. Compared to previous works of generating hand poses with a given object, we aim to allow the generalization of both hand and object shapes by a single model. Our proposed method Multi-modal Grasp Diffusion (MGD) learns the prior and conditional posterior distribution of both modalities from heterogeneous data sources. Therefore it relieves the limitation of hand-object grasp datasets by leveraging the large-scale 3D object datasets. According to both qualitative and quantitative experiments, both conditional and unconditional generation of hand grasp achieve good visual plausibility and diversity. The proposed method also generalizes well to unseen object shapes. The code and weights will be available at <https://github.com/noahcao/mgd>

*

1. Introduction

In this paper, we focus on the synthesis of static hand grasps. Instead of fitting to a small set of objects presented in certain 3D hand-object interaction datasets, we wish to generalize to diverse object geometries. We build a multi-modal generative model, capable of generating the hand poses either conditional to or jointly with the object shapes. Our model can learn to grasp objects in a pure geometric perspective instead of requiring additional conditions such as language descriptions or category labels.

Existing works [7, 14, 26] for hand-object grasp generation typically relies on datasets with *full-stack* 3D annotations [7, 26, 33]. Moreover, existing datasets are designed for different purposes in animation and robotics. Their grasp annotations are constrained to certain hand parametric models [1, 12, 16, 23, 26, 30, 33], which prevents combining different data resources. Compared to the hand model [30] for robotic manipulation, MANO [23] is a non-rigid hand model with blend skinning, requiring more details, flexibility and degree of freedom. Thus, though large-

scale synthetic datasets [30] are available for certain hand models, the datasets compatible with the MANO parametric model still suffer from limited scale and availability due to the difficulty of scanning and multi-view captures. On the other hand, human beings can transfer a grasping pattern to different objects and make plausible grasping choices for an unseen or even imagined object based on the object’s geometry. We call such ability *universal grasp generation*. Though *full-stack* 3D annotation is limited, we have large-scale 3D object datasets available. Therefore, in this work, we aim to study if we can combine the large-scale 3D object datasets to help hand-object grasp generation by jointly modeling hand and object representations in a latent space. Specifically, our model can accept grasping data with *partial supervision* in training, such as hand pose and object shape whichever are available, which significantly increases the datasets it can use for learning. Our model can generate either the full 3D grasping scenes with both the posed hand and object or a posed hand conditioned on a given object geometry. We believe such a flexible hand-object interaction generation ability without domain-specific auxiliary information makes one step forward for human-like universal grasp generation.

Following such an intention, we propose our Multi-modal Grasp Diffusion (MGD) model. It follows the latent diffusion model [22] (LDM) to encode and ensemble different modalities into a latent space and then generate plausible samples by the probabilistic denoising process [11]. To learn from more diverse objects, we construct the model by leveraging the object shape encoding and decoding networks pre-trained on the large-scale generic 3D object shape dataset [4]. As we aim to derive a universal grasp generation solution, we remove the category-specific information when constructing the latent code for objects and encode the object shapes in a purely geometric fashion.

As the hand articulation and positions are always coupled to the object shape in hand-object interaction, we design the latent diffusion to denoise the latent code from different modalities as a whole. However, we also need to decouple each modality’s representation to allow the model training by fusing data from different resources with heterogeneous annotations. Therefore, our method has indepen-

*The work in this paper was done by Jinkun Cao during his internship at Adobe in 2023 summer

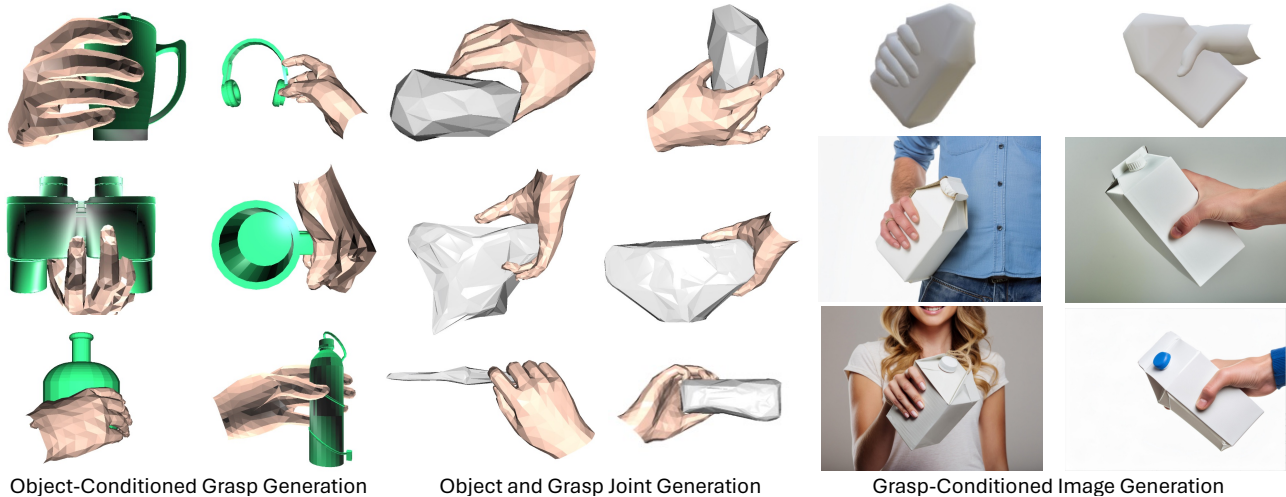


Figure 1. Applications of our proposed method Multi-modal Grasp Diffusion (MGD). Left: generating the hand grasp on an unseen object. Middle: jointly sampling a combination of the hand and the object for a plausible grasp. Right: the generated grasp can be used as guidance for generating photo-realistic grasping images using existing image generation tools [2].

dent encoder and decoder networks for different modalities and can optimize the generation of each modality solely. Such a design solves the limitation of object diversity in hand-object interaction datasets as we could leverage the data from generic object shape datasets to tune the object generation part. To achieve a certain disentanglement of modality representations, we propose to use asynchronous denoising schedulers for different modalities during noise diffusion and denoising in training. We believe we are the first to use such a strategy to solve the training stability problem raised by data with unpaired and heterogeneous annotations.

To conclude, we develop a multi-modal hand grasp generation model to sample from either joint distribution for both hand and object or the object-conditioned distribution for hand generation. It has the advantage of incorporating training resources with different annotations. By the qualitative and quantitative evaluations, our proposed method shows a good performance for grasp generation in both unconditional and object-conditioned settings. Thanks to the posterior generation learned from rich data resources, it shows significantly better performance in generating grasp over out-of-domain object shapes, which is critical for universal grasp generation. Considering that no published works have supported the generation of both hand and object to form a grasp in an end-to-end fashion, we believe our work is pioneering for the universal grasp generation task.

With the flexibility to generate both modalities in hand grasp, our model can facilitate many downstream applications. The grasps are good references to generate photo-realistic images with good geometry alignment and significantly fewer artifacts. We first generate grasps in 3D

and use them as conditional signals for image generation can help produce high-quality hand images with challenging gestures and view angles. We demonstrate using grasp from our model as the condition improves grasp alignment on images and relieves artifacts. Some examples of object-conditioned grasp generation, joint generation, and image generation with grasp rendering are presented in Figure 1. The main contribution of this work is to propose a generative model capable of generating hand grasp in either unconditional or object-conditioned fashions and the corresponding strategy to enhance the performance with limited available 3D hand-object grasp annotations.

2. Related Works

Hand Grasp Generation. Modern generative models [11] are recently introduced into hand grasp reconstruction [34] and generation. Hand grasp reconstruction asks for hand grasp rendering aligned with images while hand grasp generation asks for hand grasp visually or physically plausible. GrabNet [26] is a commonly used method for hand grasp generation but it can hardly be generalized to diverse object shapes. HOIDiffusion [38] uses the 3D hand grasp from GrabNet and an image diffusion model to generate hand-object interaction images. AffordanceDiffusion [35] also studies the generation of hand-object interaction for image synthesis. Instead of generating hand-object interaction images or videos, we focus on improving hand-object interaction in 3D space. Many recent works are based on diffusion models [5, 14, 36] or physics-based simulators [15, 31, 37]. Compared to existing works which typically require a given object [26, 35, 38, 39] shape as input, we desire generating a hand grasp over a given object or generating both the object

and hand to form a plausible grasp.

Multi-Modal Generation. With the rise of diffusion models, multi-modal generation has been extended in many areas, such as image+text generation [3] and audio+pixel generation [24]. Recently, a concurrent work UGG [14] studies to generate both hand and object to form a grasp but it uses the ShadowHand parametric model to leverage the large-scale synthetic ShadowHand grasping datasets [30] and the final results are optimization-based instead of directly from the generative model. On the other hand, another concurrent work G-HOP [36] builds a multi-modal hand-object grasp prior by encoding object shape and hand poses into a unified latent space but a language prompt is required to provide necessary conditional information. In this work, we focus on building a multi-modal diffusion model to generate the modalities of a 3D object and hand at the same time without requiring optimization or auxiliary conditions. The hand grasp is purely geometric-based. It allows more flexibility for downstream tasks, such as generating photo-realistic images by using the rendering of generated 3D hand-object interaction as a condition.

3. Method

In Section 3.1, we first provide the formal problem formulation. We then review the related preliminary knowledge for methodology and data representation in Section 3.2. Finally, we introduced our proposed method in Section 3.3.

3.1. Problem Formulation

An instance of hand-object interaction consists of a posed hand, denoted as \mathbf{H} , and a posed object, denoted as \mathbf{O} . To learn the relationship between hand gestures and object shapes, we model the joint distribution of hand and object:

$$\{\mathbf{O}, \mathbf{H}\} \sim \mathcal{D}_\Phi. \quad (1)$$

Also, in the community of visual perception, animation, and robotics, people are also interested in generating hand grasp on certain objects, which can be formulated as

$$\{\mathbf{H}\} \sim \mathcal{D}_\Phi | \mathbf{O}_g, \quad (2)$$

where \mathbf{O}_g is a provided object shape. In the previous works, the unconditional generation has been under-explored. And stand-only models for conditional hand grasp generation are usually required with no flexibility for object shape generation. Stand-only models suffer from bad robustness to different object shapes and grasp diversity. This is because existing datasets with 3D annotations of both modalities are notoriously limited in covered object shapes due to the expansiveness of scanning the object shape and capturing the corresponding hand poses. In contrast, we aim to solve both scenarios by a single model. During training, this model can adapt to any supervision which maximizes the utilization of available data.

3.2. Preliminaries

3.2.1 Latent Diffusion

Our method follows the latent diffusion models (LDM) [22, 25] to generate samples in two modality spaces, i.e., articulable hands, and rigid objects. LDM diffuses and denoises in a latent space instead of on the raw data representations.

To diffuse a data sample, given a clean latent code z_0 from a data sample $y \sim \mathcal{D}_y$, i.e., $z_0 = \mathcal{E}(y) \sim \mathcal{D}_z$, we add noise following a Markov noise process:

$$q(z_t | z_{t-1}) = \mathcal{N}(\sqrt{\alpha_t} z_{t-1}, (1 - \alpha_t)I), \quad t \in [1, T], \quad (3)$$

where $\alpha_t \in (0, 1)$ are constant hyper-parameters determined by the time step t and a noise scheduler. Though the typical diffusion model [11] trains a denoiser to predict the noise added per time step during the diffusion stage, there is another line of diffusion models [21, 28] that learns to recover the clean data sample directly. The loss turns to

$$L_{\text{LDM}} := \mathbb{E}_{z_0 \sim \mathcal{D}_z, t \sim [1, T]} \left[\|z_0 - G_\Phi(z_t, t)\|_2^2 \right], \quad (4)$$

requiring a generative model G_Φ to predict a clean latent code conditioned to a noisy latent code on a corresponding time step. We follow this paradigm of training diffusion models in this work. Besides the diffusion model itself, we also need the conversion between the raw data representation and the latent code. After recovering a clean code \hat{z}_0 , we can convert it to the raw data representation by a decoder network \mathcal{X} which is trained to be the inverse of \mathcal{E} , i.e., ideally $\mathcal{X}(z_0) \sim \mathcal{D}_y$. Therefore, there are three modules with learnable weights: an encoder network \mathcal{E} , a decoder network \mathcal{X} , and the denoiser network G_Φ .

3.2.2 Modality Representations

Here we introduce the raw representations of the modalities involved in interrupting a hand-object interaction.

Hand. We follow the MANO [23] parametric model to represent hands. Compared to another parametric model ShadowHand [1], MANO is designed for animating non-rigid real human hands instead of robotic hands thus a better fit for animation and photo-realistic generalization tasks. However, its higher complexity causes difficulty in grasping data synthesis. Therefore, there is no MANO-based hand grasping dataset as large-scale as the synthetic ShadowHand-based datasets [30] yet. This prevents research on the joint generation of MANO hands and objects in a straightforward supervised learning fashion. In this work, we directly use MANO parameters as joint rotation angles, i.e. $\theta \in \mathbb{R}^{48}$, instead of the joint xyz position to avoid the inverse kinematics. We also use the translation of hands $\mathbf{t}_h \in \mathbb{R}^3$. We don't stylize the hand shapes, thus we use constant mean shape parameters $\beta_0 = \mathbf{0}^{10}$ during linear

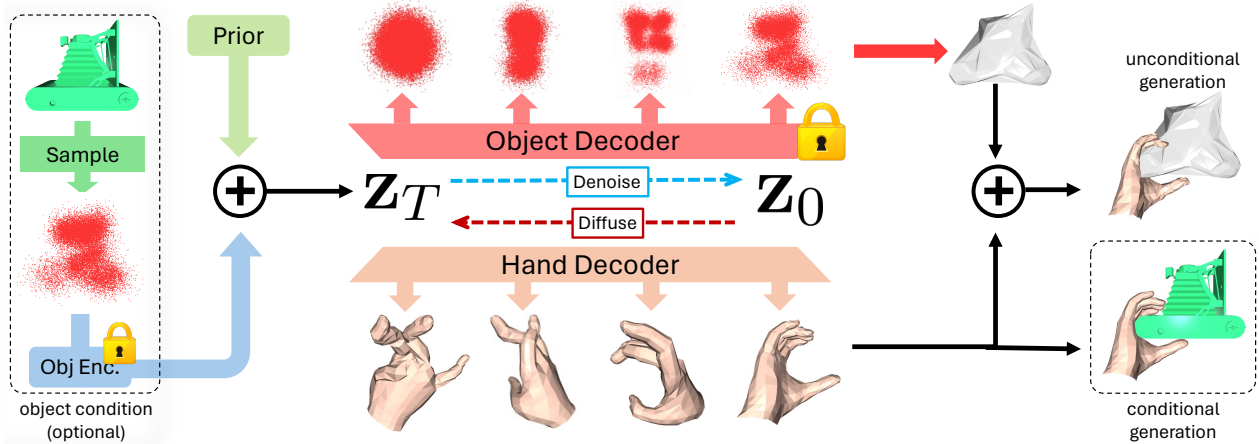


Figure 2. The illustration of our proposed Multi-modal Grasp Diffusion model (MGD). We present the main modules of the model while removing the secondary modules for simplicity. The optional object condition can turn the generation into object-conditioned.

blend skinning. The parameters of hands are concatenated and encoded by a hand encoder \mathcal{E}_H to be the hand latent code $\mathbf{y}_H \in \mathbb{R}^{51}$.

Object. For object representation, we use the point cloud latent code as $\mathbf{y}_O = \mathbf{h} \in \mathbb{R}^{N \times 4}$, where N is the number of points. As the grasp is modeled in the object-centric frame, no translation or orientation is required in the object pose and shape representation anymore. This convention is aligned with the definition of data in many hand-object grasp datasets, such as OakInk [33].

3.2.3 Object Generation

The limited amount and high category-specific bias of the objects in hand-object interaction (HOI) datasets prevent learning robust and generalizable grasps. By leveraging the large-scale object-only 3D datasets, we can derive a more robust object encoding for the grasp generation than learning from the HOI datasets solely. For the object encoding and generation part, we borrow the point-cloud-based object shape generation method LION [29]. Existing HOI generation methods can only learn object shapes from HOI datasets, including only dozens of objects, while LION learns from a much larger basis, i.e., more than 50,000 objects in ShapeNet [4]. LION proposes a Hierarchical Latent Point Diffusion Model to generate objects in two stages. In the first step, it derives a global latent code $\mathbf{z}_0^G \in \mathbb{R}^{D_G}$ from a posterior distribution $q_\phi(\mathbf{z}_0^G | \mathbf{P})$ where $\mathbf{P} \in \mathbb{R}^{u \times 3}$ is the object point cloud. Then it samples a point cloud latent \mathbf{h}_0 from a posterior $q_{\mathcal{E}_O}(\mathbf{h}_0 | \mathbf{P}, \mathbf{z}_0^G)$. LION generates the object shape by a reverse process from sampled latent code

$$p_{\mathcal{E}_O, \psi, \gamma}(\mathbf{P}, \mathbf{h}_0, \mathbf{z}_0^G) = p_{\mathcal{X}_O}(\mathbf{P} | \mathbf{h}_0, \mathbf{z}_0^G) p_\psi(\mathbf{h}_0 | \mathbf{z}_0^G) p_\gamma(\mathbf{z}_0^G), \quad (5)$$

where \mathcal{X}_O is the decoder network, ψ is the generator of point cloud latent code and γ is the distribution of global

latent code. In this work, we remove the global latent code from LION to consider the object shape from a purely geometric perspective. We encode and decode the object between point clouds and latent code from the point cloud latent \mathbf{h}_0 only. We convert the object generation part to

$$p_{\mathcal{E}_O, \psi'}(\mathbf{P}, \mathbf{h}_0) = p_{\mathcal{X}_O}(\mathbf{P} | \mathbf{h}_0) p_{\psi'}(\mathbf{h}_0), \quad (6)$$

where ψ' is fine-tuned from ψ by replacing the global prior γ with a standard Gaussian. Thanks to the pre-training from large-scale object datasets [4], we could use the weights of \mathcal{E}_O and \mathcal{X}_O from LION directly. By freezing the encoder and decoder, we fine-tune the object prior distribution with the object shapes from HOI datasets. In this fashion, the model provides a robust object encoding for the latent diffusion model and keeps the sampled object shapes proper for the single-hand interaction.

3.3. Multi-modal Grasp Diffusion (MGD)

We now introduce our proposed Multi-modal Grasp Diffusion (MGD). We present the overall illustration and key designs of our proposed method in Figure 2.

3.3.1 Latent Codes for Different Modalities

For each modality aforementioned, we have an MLP-based encoding network to convert the raw representation into latent codes:

$$\mathbf{z}_0^H = \mathcal{E}_H(\mathbf{y}_H), \quad \mathbf{z}_0^O = \mathcal{E}_O(\mathbf{y}_O), \quad (7)$$

with the dimensions $\mathbf{z}_0^H \in \mathbb{R}^{1 \times 512}$ and $\mathbf{z}_0^O \in \mathbb{R}^{4 \times 512}$. They are concatenated to be the final latent code for the whole hand-object interaction configuration

$$\mathbf{z}_0 = \mathbf{z}_0^H \oplus \mathbf{z}_0^O \in \mathbb{R}^{5 \times 512}. \quad (8)$$

This design allows us to jointly process different modalities without unnecessary entanglement. This allows us to train the model with partial modality supervision without corrupting the parameters for other modalities.

3.3.2 Asynchronous Denoising Schedulers

We propose to generate either both hand and object or only the hand given an object shape. To realize this, we need a certain degree of entanglement between the two modalities as we need them to cooperate to form a valid grasp. However, we still desire certain isolation so that we could supervise the model training with partially annotated data, for example only the 3D object shapes. In the usual fashion of organizing multi-modal latent codes in latent diffusion models, the latent codes of different modalities always have the same level of noise corruption as they share a single noise scheduler. However, we desire the two modalities can be denoised with respect to an arbitrary level of noise in the other modality. Therefore, we propose to use asynchronous denoising schedulers for this purpose during training. Instead of using a single noise scheduler, we have two schedulers t_H and t_O to control the noise patterns in the hand latent code and the object latent code respectively. Following Equation (3) we derive the corrupted latent codes as

$$\mathbf{z}_{t_H}^H = \prod_{t=1}^{t_H} q(\mathbf{z}_t^H | \mathbf{z}_{t-1}^H), \quad \mathbf{z}_{t_O}^O = \prod_{t=1}^{t_O} q(\mathbf{z}_t^O | \mathbf{z}_{t-1}^O), \quad (9)$$

with the same time step range $t_O, t_H \in [1, T]$. This design enables the diffusion to deal with the noise in each modality separately. During training, it allows using object-only data to supervise the object part only. During sampling, it allows the model to generate only the hand given an object shape as the condition. Similar to Bao et al. [3], we will learn the joint distribution for hand-object pairs and the marginal distribution for the hand at the same time in an end-to-end fashion by manipulating the time schedulers.

3.3.3 Training and Sampling

Now we introduce the training and sampling paradigm of MGD. There are two main goals in designing it. First, we would like to use the training with heterogeneous annotations so that we can go beyond the limited object shapes in HOI datasets. Second, we want a single model capable of object-conditioned hand grasp generation and unconditional hand-object joint generation.

Training. When training on the canonical HOI data samples, with the asynchronous noise schedulers, we can derive the assembly of two corrupted latent codes as

$$\mathbf{z}_{t_H, t_O} = \mathbf{z}_{t_H}^H \oplus \mathbf{z}_{t_O}^O. \quad (10)$$

Due to the element-wise property of MSE loss used for diffusion model training, we can calculate and back-propagate

the gradient to a certain part of the latent codes independently. We leverage this property to train the unconditional and conditional generation at the same time. First, we learn the joint distribution by the unconditional generation loss

$$L_{\text{uncond.}} = \mathbb{E}_{z_0 \sim \mathcal{D}_{HO}, \{t_H, t_O\} \sim [1, T]} \left[\|z_0 - G_{\Phi}(z_{t_H, t_O}, t_H, t_O)\|_2^2 \right], \quad (11)$$

where \mathcal{D}_{HO} is the distribution of the HOI datasets [26, 33].

Also, we train the model to learn the object-conditioned grasp generation. In this situation, the object latent code is given and fixed as \mathbf{z}_0^O and we set $t_O = 0$ indicating that the object part is noise-free and serves as a condition to derive the marginal distribution now. We now train with the loss

$$L_{\text{cond.}} = \mathbb{E}_{z_0 \sim \mathcal{D}_{HO}, t_H \sim [1, T]} \left[\|z_0 - G_{\Phi}(z_{t_H}, t_H)\|_2^2 \right], \quad (12)$$

with

$$t_O = 0, \quad z_{t_H} = z_{t_H}^H \oplus \mathbf{z}_0^O. \quad (13)$$

The conditional and unconditional generation losses require uncorrupted and corrupted object latent codes respectively. In practice, we combine these two training objectives in a 1:1 ratio for a single draw of the training data batch. This training strategy is similar to the classifier-free guidance [10] for diffusion model training. However, the optional condition (object) exists in the input and output latent instead of in an independent condition vector.

Finally, we could leverage the large-scale 3D object shape datasets to train the object distribution only. This is done by selecting object samples from a wider source of datasets as we do not need available hand grasps over them anymore. The loss turns to

$$L_{\text{obj.}} = \mathbb{E}_{z_0^O \sim \mathcal{D}_O \cup \mathcal{D}_{HO}, t_O \sim [1, T]} \left[\|z_0 - G_{\Phi}(z_{t_O}, t_O)\|_2^2 \right], \quad (14)$$

where \mathcal{D}_O is object-only datasets. The latent codes only take the object part as the variable:

$$\mathbf{z}_0 = \epsilon \oplus \mathbf{z}_0^O, \quad \mathbf{z}_{t_O} = \epsilon \oplus \mathbf{z}_{t_O}^O, \quad s.t. \quad \epsilon \sim \mathcal{N}(0, I). \quad (15)$$

Obviously, the gradient only influences the object-related parts while keeping the hand part as-is. During training, the object encoder and decoder networks are pre-trained on the ShapeNet [4] and frozen. All other encoder, decoder, and denoiser networks are trained end to end.

Similar to the proximity sensor features [27] and the Grasping Filed [13], we use a distance field to help capture the relation between the hand and the object. Since we eliminate the requirement of object templates to accommodate more general datasets, we can not define the field using object keypoints [7] or templated vertices. Instead, we define the distance field as the vectors between each hand joint and the 10 closest points in the object points. Therefore, we have the distance field as $\mathbf{y}_f \in \mathbb{R}^{16 \times 30}$. When the data

sample is drawn from HOI datasets, we would also supervise the distance field calculated from the recovered hand gesture and object shape:

$$L_{\text{distance}} = \|\mathbf{y}_f - \hat{\mathbf{y}}_f\|_2^2, \quad (16)$$

Besides supervision of the raw MANO parameters for hand, we also supervise the joint position by the loss

$$L_{\text{hand.xyz}} = \|\text{LBS}(\mathbf{y}_H) - \text{LBS}(\hat{\mathbf{y}}_H)\|_2^2, \quad (17)$$

where $\text{LBS}(\cdot)$ is the linear blend skinning process by MANO parametric model to derive the joint kinematic positions. With all the losses introduced, we could train the multi-modal diffusion model using data with heterogeneous annotations and for unconditional and conditional generation at the same time. The overall loss is

$$L = \mathbb{1}_{z_0 \sim D_{HO}} (L_{\text{uncond.}} + L_{\text{cond.}} + L_{\text{distance}} + L_{\text{hand.xyz}}) + L_{\text{obj.}}, \quad (18)$$

where $\mathbb{1}_{z_0 \sim D_{HO}}$ indicates whether the data sample is drawn from a HOI dataset.

Sampling. We follow the canonical progressive denoising process for diffusion models in the sampling stage. To sample for joint (unconditional) HOI generation, we synchronize the schedulers $t_H = t_O = t$. Similar to Tevet et al. [28], at each step t , we predict a clean sample by $\hat{z}_0 = G_{\Phi}(z_t, t_H, t_O)$ from the corrupted code z_t and then noise it back to z_{t-1} . During sampling for object-conditioned grasp generation, we keep $t_O = 0$ and $z_{t_H} = z_{t_H}^H \oplus z_0^O$. Then the denoiser predicts $\hat{z}_0 = G_{\Phi}(z_{t_H}, t_H)$ and then noise it back to z_{t-1} . In either the unconditional or the conditional generation, we repeat the process above along $t = T \rightarrow 1$ until the final \hat{z}_0 is achieved after T iterations.

4. Experiments

4.1. Setups

Datasets. The hand-object interaction (HOI) datasets usually face limitations of the diversity of object shapes. We combine the data from multiple resources to train the model. GRAB [26] contains human full-body poses together with 3D objects. We extract the hands from the full-body annotations. For OakInk-Shape [33], we use the official training split for training. We also use the contact-adapted synthetic grasp on the OakInk-Shape set for training. Besides the hand-object interaction data, we also leverage the rich resources of 3D object data to help train the object part in our model. The object data is also used to train the LION code prior distribution as the original distribution (pre-trained from ShapeNet [4]) can produce object shapes that are not proper for single-hand grasp, for example, sofa, chair, and bookcase. We combine the objects from GRAB, OakInk (both the objects from OakInk-Image with grasp annotation and the objects from OakInk-shape without grasps),

Affordpose [35] and DexGraspNet [30] as the object data resource. We also leverage the DeepSDF [18] as trained in Ink-base [33] to provide synthetic object data and include them in OakInk-Shape. To evaluate the generation quality on unseen objects, we leave the ARCTIC [7] dataset away from training and only used for evaluation purposes. Please refer to the supplemental for the statistics of each dataset.

Data Pre-Processing. We follow the convention in OakInk-Shape to transform the hands into the object-centric frame. For data from GRAB [26], we extract the MANO parameters from its original SMPL-X [19] annotations. Then, we filter out the frames where the right-hand mesh has no contact with the object in training. For the object representation, we randomly sample 2048 points from mesh vertices to represent each object. For the objects in the OakInk-Shape dataset, we sample the point clouds from the object mesh surfaces uniformly instead of sampling from the vertices because the annotated mesh vertices are too sparse on smooth surfaces.

Implementation. The DeepSDF in Ink [33] is trained per category to derive better details and fidelity when interpolating object shapes. We use the DeepSDF to provide synthetic object shapes. For the tokenizer network (transforming modality features to latent codes), we always use 2-layer MLP networks with a hidden dimension of 1024 and an output dimension of 512. For the denoiser, we follow MDM [28] to use a transformer encoder-only backbone-based diffusion network. After decoding the object latent code by the LION decoder, we derive the point cloud set. For visualization purposes, we conduct surface reconstruction from the generated object point cloud. Though advanced surface reconstruction techniques such as some learned solver [20] can provide more details, this part is not our focus and we wish to keep consistency for out-of-domain objects generated. Therefore, we choose the naive Alpha Shape algorithm [6].

Evaluation and Metrics. Unlike the reconstruction tasks where the ground truth is available, it is difficult to do the quantitative evaluation for generation models. We keep the OakInk-Shape test set for quantitative evaluations and follow its metrics set. Referring to the evaluation of image generation quality, we first measure the quality of generated grasp by FID (Frechet Inception Distance) [9] between the images rendered from the ground truth grasps and the generated grasps. We can not directly calculate the FID score on generated 3D parameters as there is no commonly used encoder for this purpose and implementing it ourselves can cause many ambiguities. We also measure the model performance by directly checking the 3D asset quality. We follow previous studies [32, 33] to use three metrics: (1) the penetration depth (Pene. Depth) between hand and object mesh, (2) the solid intersection volume (Intsec. Vol.) between them and (3) the mean displacement in simulation

Table 1. Quantitative evaluation of grasp generation. The top four entries are evaluated on objects from the OakInk-test set. The bottom two entries are evaluated on the same set of objects generated from MGD in the unconditional mode, which are out of the domain from the objects seen during training.

Objects	Methods	FID ↓	Pene. Dep. ↓	Intsec. Vol. ↓	Sim. Disp. Mean ↓	User Scor. ↑
OakInk-test	GrabNet [26]	26.96	0.70	11.93	3.14	3.80
	GrabNet-Refine [26, 33]	25.26	0.63	4.44	2.78	4.00
	MGD	20.73	0.32	3.87	2.52	4.87
Self-generated	GrabNet-Refine	-	1.17	13.82	10.03	1.33
	MGD(uncond.)	-	0.51	6.71	7.13	3.53

Table 2. The ablation study about the impact of training data on the generation quality over unseen objects from ARCTIC [7]. Adding more training data consistently boosts the generation quality on unseen objects.

OakInk-Shape	GRAB	Object-only Data	FID ↓	Pene. Dep. ↓	Intsec. Vol. ↓	Sim. Disp. Mean ↓	User Scor. ↑
✓			27.29	0.51	4.89	3.22	3.87
✓	✓		25.31	0.47	4.61	3.08	4.00
✓	✓	✓	23.92	0.42	4.55	2.91	4.13

following [8]. Finally, we perform a user study to measure the plausibility and the truthfulness of the generated grasps by scoring (1-5). We invite 15 participants to rate the quality of batches of the mixture of 10 rendering of ground truth grasps and 10 generated grasps. The score 1 indicates “totally fake and implausible” and 5 indicates “plausible enough to be real”. Each participant evaluates by averaging the scores over 10 randomly selected batches.

4.2. Object-Conditioned Grasp Generation

We select the objects from OakInk-Shape test sets to generate grasps on them. Our method can generate visually plausible grasp configurations even though the model has not seen these objects during training.

We perform the quantitative evaluation on the OakInk-Shape test set with the previously introduced metrics. We follow the previous practice [33] to use the widely adopted GrabNet [26] and its refined version GrabNet-refine [33] as the baseline models. We train the models on the GRAB and OakInk-shape train splits. The results are shown in Table 1. Compared to the baseline methods, our proposed method achieves better generation quality per four metrics: FID, Mesh Penetration Depth, Intersection Volume, and Mean Simulation Displacement. Significantly, it achieves nearly 50% improvement regarding the penetration depth. Per the plausibility and truthfulness rated by invited participants, our method also achieves a better rating. Our method achieves a convincingly good performance. Moreover, when we use the objects generated by our method itself, its performance advantage over GrabNet is more significant. This is probably because GrabNet is harder to generalize to object shapes that are significantly different from its training data. On the other hand, as our method learns more generalizable and diverse object prior information by modeling objects in a pure geometric perspective, its robust-

ness to diverse object shapes is much better.

4.3. Unconditional Grasp Generation

Unconditional grasp generation is a main contribution of this work. Without the massive scale of full-stack datasets such as synthetic robotic manipulation datasets [30], our method is still capable of doing this. It learns the joint distribution between the latent representation of hand and object and leverages the large-scale object datasets to learn a sufficiently generalizable object shape representation model. Compared to the objects generated by the original LION, our method generates objects that are more proper for hand-object interaction after fine-tuning the object prior distribution by the object samples from the selected datasets. We selected some samples from the unconditional grasp generation in the supplementary. We also conduct the quantitative evaluation for the unconditional generation quality by MGD. The results are shown in Table 1. The baseline GrabNet suffers from generating plausible grasps on the out-of-distribution object shapes while our method achieves good results. Moreover, it even achieves on-par performance compared to the generation quality of the baseline GrabNet in the object-conditioned setting, which is very impressive. By learning from large-scale object datasets, the ability of our method to generate object shapes and hand grasp at the same time gives a unique advantage. We think this is a key capacity for the universal grasp generation. Compared to the object-conditioned generated grasps from MGD, the quality of unconditional generation is inferior, which is in fact as expected. This reveals a limitation of existing hand-grasp synthesis methods in many situations. Because the HOI datasets, e.g., OakInk and DexGraspNet [30], usually contain objects from certain categories, with similar scale, geometry, and affordance, the method trained on the training split can learn significantly biased in-domain knowledge

Table 3. The ablation study about the impact of training data on the generation quality for joint generation of hand and object. Adding more data, either hand-object grasp data or object-only data, improves the generation quality.

OakInk-Shape	GRAB	Object-only Data ↓	Pene. Dep. ↓	Intsec. Vol. ↓	Sim. Disp. Mean ↓	User Scor.↑
✓			0.92	8.12	8.23	3.33
✓	✓		0.51	6.71	7.13	3.53
✓	✓	✓	0.43	5.55	6.98	3.73

Table 4. Ablation about asynchronous denoising schedulers. We evaluate on the generated object shapes by MGD.

Asyn.	Pene. Dep. ↓	Intsec. Vol. ↓	Sim. Disp. Mean ↓
	0.57	6.52	7.88
✓	0.43	5.55	6.98

about the objects in the test splits. However, a typical object generation model, which is trained on much larger-scale and more diverse object shape datasets, can generate objects with significantly different scales, geometries, and topologies. To generate hand grasps on these out-of-domain object shapes would be a challenge to all existing methods. By designing the method capable of training with object-only data and disentangling the modality representations in the latent diffusion, our method not only has the advantage of generating the object and the hand grasp simultaneously but also achieves much better robustness to generate grasps on out-of-domain objects.

4.4. Ablation Study

During training, we fuse multiple datasets with heterogeneous annotations to gain as rich object shape and grasp data as possible. This shows the flexibility of our method to be trained with different supervision. However, it also introduces additional variance and potential noise to measure the performance contribution from our methodology. Therefore, we provide ablation studies here to better understand the method’s performance.

Ablation of grasp generation on unseen objects. To provide transparent experimental conclusions, we ablate the training data on the model generation quality. Because OakInk-train data is used for training, which can be biasedly similar to the OakInk-test split, we use the objects from ARCTIC [7] to measure the conditional generation quality on unseen objects. The quantitative evaluation results are shown in Table 2. Compared to using only OakInk-Shape data for training, adding GRAB data and object shapes from Object-only datasets both improves the generalization qualities. The improvement from extra GRAB data is easy to explain as training with more data usually improves the generalizability of the model. It is interesting that adding the object-only datasets also boosts the performance. We believe this is because the extra object data improves the robustness and generalizability of the object encoding and representation modules. It improves the latent representa-

tion that the diffusion model learns to generate.

Ablation of unconditional generation quality. The ability to generate both hand and object to form a grasp is another main contribution. We are interested in whether it can benefit from the additional training data as well. We present the ablation study in Table 3. Similar to the conditional generation ablation study results, the unconditional generation quality also benefits from additional training data consistently. The metrics of Pene. Dep., Intsec. Vol. and Sim. Disp. Mean indicate that the generated hand-object pair improves plausibility along with adding more training data. The increasing user scoring result suggests that the generated object and hand also become more and more visually realistic along with adding more training data.

Ablation of synchronous denoising schedulers. As one of the main implementation innovations of MGD, we conduct an ablation about Asynchronous Denoising Schedulers in Table 4. Intuitively, we designed this module to decouple the noise level in hand latent and object latent so that the model could better use the data with heterogeneous annotations and learn to denoise a certain modality. Without Asynchronous Denoising Schedulers, the noise diffusion and denoising time step of the object part is always correlated to the hand latent code. It makes the training biased to the HOI dataset where both modalities are available for supervision. Adding Asynchronous Denoising Schedulers, the denoising is learned with more independence for the object part and the hand part. The model can better learn object shape coding to generate hand grasps. Therefore, when evaluating on the out-of-domain objects generated by MGD, the generation quality is improved as expected.

5. Conclusion

In this work, we propose a multi-modal grasp diffusion model. By encoding the modalities of objects and hands into a unified latent space, we could generate them either jointly or conditionally. We reveal the limitations of training and test generation quality within the domain and explore how to learn grasp generation on universal objects. Our model can benefit from data with partial annotation thus relieving the limitation of full-stack annotated 3D hand-object grasp data. Neither auxiliary information such as category labels or text descriptions nor optimization is needed in our proposed method. The generated grasp in both unconditional and conditional settings shows good quality.

References

- [1] Dexterous hand series.
- [2] Adobe. Firefly, 2024. <https://www.adobe.com/products/firefly.html>.
- [3] Fan Bao, Shen Nie, Kaiwen Xue, Chongxuan Li, Shi Pu, Yaole Wang, Gang Yue, Yue Cao, Hang Su, and Jun Zhu. One transformer fits all distributions in multi-modal diffusion at scale. *arXiv preprint arXiv:2303.06555*, 2023.
- [4] Angel X Chang, Thomas Funkhouser, Leonidas Guibas, Pat Hanrahan, Qixing Huang, Zimo Li, Silvio Savarese, Manolis Savva, Shuran Song, Hao Su, et al. Shapenet: An information-rich 3d model repository. *arXiv preprint arXiv:1512.03012*, 2015.
- [5] Sammy Christen, Shreyas Hampali, Fadime Sener, Edoardo Remelli, Tomas Hodan, Eric Sauser, Shugao Ma, and Bugra Tekin. Diffh2o: Diffusion-based synthesis of hand-object interactions from textual descriptions. *arXiv preprint arXiv:2403.17827*, 2024.
- [6] Herbert Edelsbrunner, David Kirkpatrick, and Raimund Seidel. On the shape of a set of points in the plane. *IEEE Transactions on information theory*, 29(4):551–559, 1983.
- [7] Zicong Fan, Omid Taheri, Dimitrios Tzionas, Muhammed Kocabas, Manuel Kaufmann, Michael J Black, and Otmar Hilliges. Arctic: A dataset for dexterous bimanual hand-object manipulation. In *Proceedings of the IEEE/CVF Conference on Computer Vision and Pattern Recognition*, pages 12943–12954, 2023.
- [8] Yana Hasson, Gul Varol, Dimitrios Tzionas, Igor Kaleyvatykh, Michael J Black, Ivan Laptev, and Cordelia Schmid. Learning joint reconstruction of hands and manipulated objects. In *Proceedings of the IEEE/CVF conference on computer vision and pattern recognition*, pages 11807–11816, 2019.
- [9] Martin Heusel, Hubert Ramsauer, Thomas Unterthiner, Bernhard Nessler, and Sepp Hochreiter. Gans trained by a two time-scale update rule converge to a local nash equilibrium. *Advances in neural information processing systems*, 30, 2017.
- [10] Jonathan Ho and Tim Salimans. Classifier-free diffusion guidance. *arXiv preprint arXiv:2207.12598*, 2022.
- [11] Jonathan Ho, Ajay Jain, and Pieter Abbeel. Denoising diffusion probabilistic models. *Advances in neural information processing systems*, 33:6840–6851, 2020.
- [12] Juntao Jian, Xiuping Liu, Manyi Li, Ruizhen Hu, and Jian Liu. Affordpose: A large-scale dataset of hand-object interactions with affordance-driven hand pose. In *Proceedings of the IEEE/CVF International Conference on Computer Vision*, pages 14713–14724, 2023.
- [13] Korrawe Karunratanakul, Jinlong Yang, Yan Zhang, Michael J Black, Krikamol Muandet, and Siyu Tang. Grasping field: Learning implicit representations for human grasps. In *2020 International Conference on 3D Vision (3DV)*, pages 333–344. IEEE, 2020.
- [14] Jiaxin Lu, Hao Kang, Haoxiang Li, Bo Liu, Yiding Yang, Qixing Huang, and Gang Hua. Ugg: Unified generative grasping. *arXiv preprint arXiv:2311.16917*, 2023.
- [15] Zhengyi Luo, Jinkun Cao, Sammy Christen, Alexander Winkler, Kris Kitani, and Weipeng Xu. Grasping diverse objects with simulated humanoids. *arXiv preprint arXiv:2407.11385*, 2024.
- [16] Andrew T Miller and Peter K Allen. Graspit! a versatile simulator for robotic grasping. *IEEE Robotics & Automation Magazine*, 11(4):110–122, 2004.
- [17] Supreeth Narasimhaswamy, Uttaran Bhattacharya, Xiang Chen, Ishita Dasgupta, Saayan Mitra, and Minh Hoai. Hand-iffuser: Text-to-image generation with realistic hand appearances. *arXiv preprint arXiv:2403.01693*, 2024.
- [18] Jeong Joon Park, Peter Florence, Julian Straub, Richard Newcombe, and Steven Lovegrove. DeepSDF: Learning continuous signed distance functions for shape representation. In *Proceedings of the IEEE/CVF conference on computer vision and pattern recognition*, pages 165–174, 2019.
- [19] Georgios Pavlakos, Vasileios Choutas, Nima Ghorbani, Timo Bolkart, Ahmed A. A. Osman, Dimitrios Tzionas, and Michael J. Black. Expressive body capture: 3d hands, face, and body from a single image. In *Proceedings IEEE Conf. on Computer Vision and Pattern Recognition (CVPR)*, 2019.
- [20] Songyou Peng, Chiyu Jiang, Yiyi Liao, Michael Niemeyer, Marc Pollefeys, and Andreas Geiger. Shape as points: A differentiable poisson solver. *Advances in Neural Information Processing Systems*, 34:13032–13044, 2021.
- [21] Aditya Ramesh, Prafulla Dhariwal, Alex Nichol, Casey Chu, and Mark Chen. Hierarchical text-conditional image generation with clip latents. *arXiv preprint arXiv:2204.06125*, 1(2):3, 2022.
- [22] Robin Rombach, Andreas Blattmann, Dominik Lorenz, Patrick Esser, and Björn Ommer. High-resolution image synthesis with latent diffusion models. In *Proceedings of the IEEE/CVF conference on computer vision and pattern recognition*, pages 10684–10695, 2022.
- [23] Javier Romero, Dimitrios Tzionas, and Michael J Black. Embodied hands: Modeling and capturing hands and bodies together. *arXiv preprint arXiv:2201.02610*, 2022.
- [24] Ludan Ruan, Yiyang Ma, Huan Yang, Huiguo He, Bei Liu, Jianlong Fu, Nicholas Jing Yuan, Qin Jin, and Baining Guo. Mm-diffusion: Learning multi-modal diffusion models for joint audio and video generation. In *Proceedings of the IEEE/CVF Conference on Computer Vision and Pattern Recognition*, pages 10219–10228, 2023.
- [25] Jascha Sohl-Dickstein, Eric Weiss, Niru Maheswaranathan, and Surya Ganguli. Deep unsupervised learning using nonequilibrium thermodynamics. In *International conference on machine learning*, pages 2256–2265. PMLR, 2015.
- [26] Omid Taheri, Nima Ghorbani, Michael J Black, and Dimitrios Tzionas. Grab: A dataset of whole-body human grasping of objects. In *Computer Vision—ECCV 2020: 16th European Conference, Glasgow, UK, August 23–28, 2020, Proceedings, Part IV 16*, pages 581–600. Springer, 2020.
- [27] Omid Taheri, Yi Zhou, Dimitrios Tzionas, Yang Zhou, Duygu Ceylan, Soren Pirk, and Michael J Black. Grip: Generating interaction poses using spatial cues and latent consistency. In *International conference on 3D vision (3DV)*, 2024.

- [28] Guy Tevet, Sigal Raab, Brian Gordon, Yonatan Shafir, Daniel Cohen-Or, and Amit H Bermano. Human motion diffusion model. *arXiv preprint arXiv:2209.14916*, 2022.
- [29] Arash Vahdat, Francis Williams, Zan Gojcic, Or Litany, Sanja Fidler, Karsten Kreis, et al. Lion: Latent point diffusion models for 3d shape generation. *Advances in Neural Information Processing Systems*, 35:10021–10039, 2022.
- [30] Ruicheng Wang, Jialiang Zhang, Jiayi Chen, Yinzhen Xu, Puhao Li, Tengyu Liu, and He Wang. Dexgraspnet: A large-scale robotic dexterous grasp dataset for general objects based on simulation. In *2023 IEEE International Conference on Robotics and Automation (ICRA)*, pages 11359–11366. IEEE, 2023.
- [31] Sirui Xu, Zhengyuan Li, Yu-Xiong Wang, and Liang-Yan Gui. Interdiff: Generating 3d human-object interactions with physics-informed diffusion. In *Proceedings of the IEEE/CVF International Conference on Computer Vision*, pages 14928–14940, 2023.
- [32] Lixin Yang, Xinyu Zhan, Kailin Li, Wenqiang Xu, Jiefeng Li, and Cewu Lu. Cpf: Learning a contact potential field to model the hand-object interaction. In *Proceedings of the IEEE/CVF International Conference on Computer Vision*, pages 11097–11106, 2021.
- [33] Lixin Yang, Kailin Li, Xinyu Zhan, Fei Wu, Anran Xu, Liu Liu, and Cewu Lu. Oakink: A large-scale knowledge repository for understanding hand-object interaction. In *Proceedings of the IEEE/CVF Conference on Computer Vision and Pattern Recognition*, pages 20953–20962, 2022.
- [34] Yufei Ye, Poorvi Hebbar, Abhinav Gupta, and Shubham Tulsiani. Diffusion-guided reconstruction of everyday hand-object interaction clips. In *Proceedings of the IEEE/CVF International Conference on Computer Vision*, pages 19717–19728, 2023.
- [35] Yufei Ye, Xueting Li, Abhinav Gupta, Shalini De Mello, Stan Birchfield, Jiaming Song, Shubham Tulsiani, and Sifei Liu. Affordance diffusion: Synthesizing hand-object interactions. In *Proceedings of the IEEE/CVF Conference on Computer Vision and Pattern Recognition*, pages 22479–22489, 2023.
- [36] Yufei Ye, Abhinav Gupta, Kris Kitani, and Shubham Tulsiani. G-hop: Generative hand-object prior for interaction reconstruction and grasp synthesis. In *Proceedings of the IEEE/CVF Conference on Computer Vision and Pattern Recognition*, pages 1911–1920, 2024.
- [37] Hui Zhang, Sammy Christen, Zicong Fan, Otmar Hilliges, and Jie Song. Grasppl: Generating grasping motions for diverse objects at scale. *arXiv preprint arXiv:2403.19649*, 2024.
- [38] Mengqi Zhang, Yang Fu, Zheng Ding, Sifei Liu, Zhuowen Tu, and Xiaolong Wang. Hoidiffusion: Generating realistic 3d hand-object interaction data. In *Proceedings of the IEEE/CVF Conference on Computer Vision and Pattern Recognition*, pages 8521–8531, 2024.
- [39] Keyang Zhou, Bharat Lal Bhatnagar, Jan Eric Lenssen, and Gerard Pons-Moll. Gears: Local geometry-aware hand-object interaction synthesis. In *Proceedings of the IEEE/CVF Conference on Computer Vision and Pattern Recognition*, pages 20634–20643, 2024.

We provide more details about this work and visualizations in the supplementary materials, including the quantitative results, dataset statistics, and also limitation and failure cases analysis.

A. Qualitative Results

We showcase the qualitative visualization results of our proposed method here. We select the object shapes from GRAB and OakInk-Shape that are not used in training as the object condition. The generated hand grasps are presented in Figure 3 and Figure 4. On the same object or objects with similar shapes, we can observe different hand grasp patterns, which are visually plausible. Given that these object shapes are unseen during training and no text/category description is provided as an extra condition, we believe such grasping generation is made from the model’s ability to generate grasping from a pure geometric perspective of the object shape. Moreover, by sampling noise from the latent space, we could generate the object shape and a corresponding hand grasp unconditionally. The results are presented in Figure 5. We could notice the good plausibility of the generated hand-object grasp. The hand pose and articulation are well adapted to the object shapes generated. Compared to the object shapes from real-world scanning, the objects generated by our method lack the same level of well carving. This is also related to the surface reconstruction algorithm, i.e., Alpha Shape [6], which we leveraged to reconstruct mesh from point clouds. Applying a more advanced surface reconstruction method can improve the details and fidelity of the object shapes but that is out of the scope of this work. Moreover, as we study the object shapes from a pure geometric perspective, we can’t use the surface reconstruction arts that require category prior.

B. Grasp Diversity

Given a single object shape, we could generate a set of different grasps onto it. Though diversity is expected to be constrained by the hand grasp data available in training, there are some other implicit but more fundamental cues to help generate diverse hand grasp. This underlying but fundamental constraint can be leveraged to enhance the generation robustness over unseen objects if the feature of the object shape is sufficiently generalizable. For example, the model can learn to avoid penetration between the object volume and the hand shape and certain fingers should be close to the surface of objects to form a physically valid grasp. We generate grasps with unseen objects from the OakInk-shape test set as the condition in Figure 6. We observe some grasp patterns not provided in the training set, for example, holding a dagger between two fingers. As the implicit concept of forming a valid grasp is always conditioned to object shapes, our strategy of exposing the model training to more

diverse object shapes can help to learn grasp patterns on unseen and even out-of-domain objects. We believe this is a key reason for making our method outstanding when generating grasps on out-of-domain objects.

C. Dataset Statistics

Here we provide more details about the statistics of the datasets involved in our training and evaluation in Table 5. The HOI datasets with deformable and articulable hand models, i.e., MANO [23], face severe limitations of object resources. Combining the training set of GRAB [26] and OakInk-Image [33] datasets still make just ~ 100 objects. On the other hand, AffordPose [12] and DexGraspNet [30] contain more object shapes but the different choices of hand models make them hard to integrate with MANO-parameterized datasets. Fortunately, we have the large-scale 3D object shape dataset ShapeNet [4] with more than 50,000 objects. We combine the objects from these datasets in the training for the object part. They help to construct a more universal prior distribution for object generation and the grasp posterior distribution.

D. Grasp-conditioned Image Generation

We demonstrate using MGD as a creativity tool to generate 3D grasps and the corresponding images. In Figure 7, we first use MGD to sample interaction pairs of 3D hands and objects. With the rendering of the 3D hand-object grasp as the input, we applied Adobe Firefly [2], an existing tool to generate the images with the depth and edge reference of the 3D pairs. The hand pose and the geometry provide guidance for Firefly to complement the details given simple text prompts. In Figure 8, compared to grasping images authorized purely by text prompts, images guided by MGD’s output have more consistent gestures, better-aligned object geometry and boundaries, and fewer hand artifacts. Therefore, with the rise of text-to-image generation, our hand-object grasp generation model can serve as a proxy to enhance the consistency among multiple instances and the visual plausibilities. We also provide a closer look at their detailed in Figure 9 to compare the results with and without the generated grasp as a proxy. At each row, the images are generated from the same text prompt as shown at the bottom. There are two main benefits of generating images conditioned to the grasp. It first allows a set of images with aligned hand and object geometry and boundaries which can be useful for image and video editing. On the other hand, even though the Adobe Firefly generator has shown a significant advantage over the public Stable Diffusion in eliminating artifacts, we still observed many finger artifacts when generating the images without a grasp condition. Fortunately, with the generated grasp, including the object shape and the hand, as the condition, the image gen-

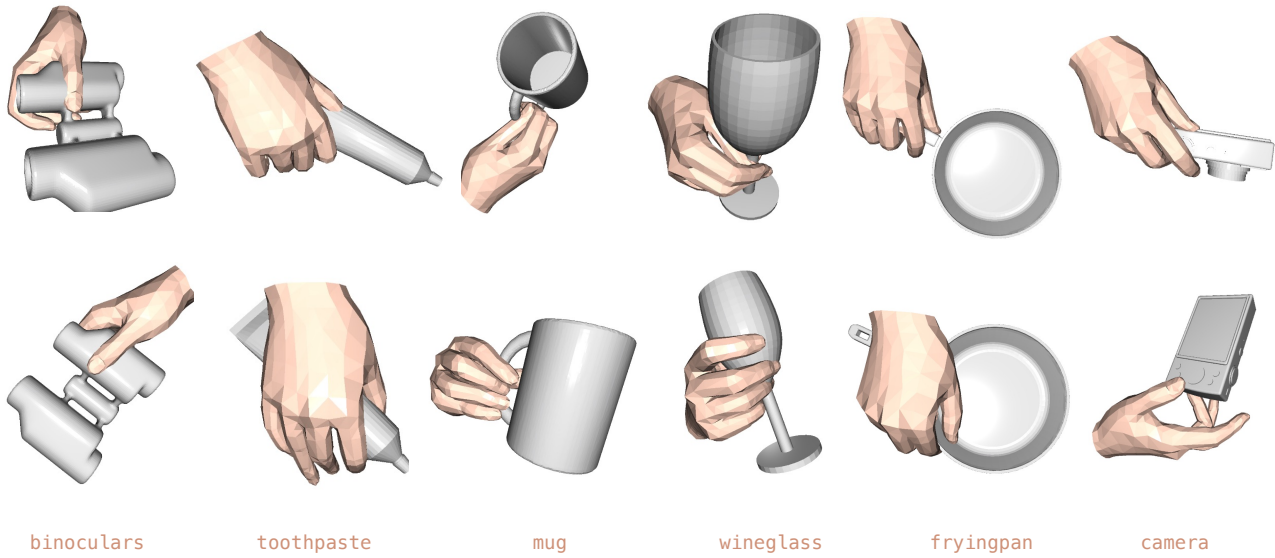


Figure 3. Samples of object-conditioned grasp generation on GRAB.

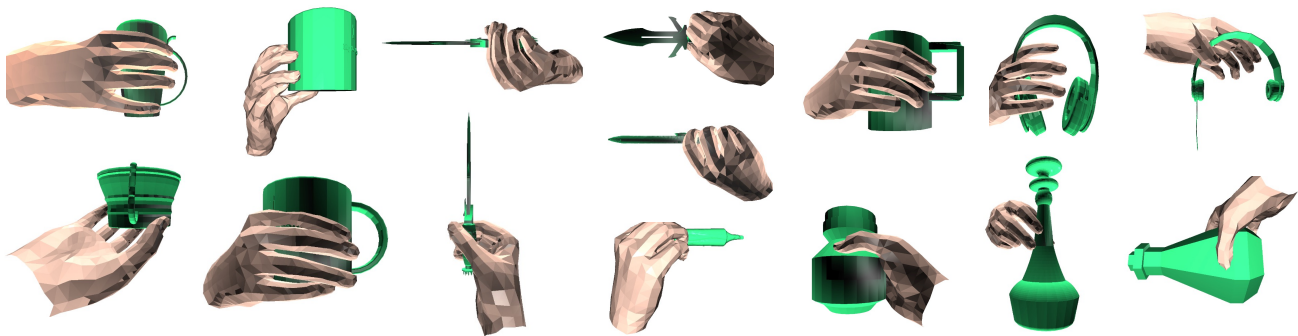


Figure 4. Samples of object-conditioned grasp generation on OakInk-Shape.

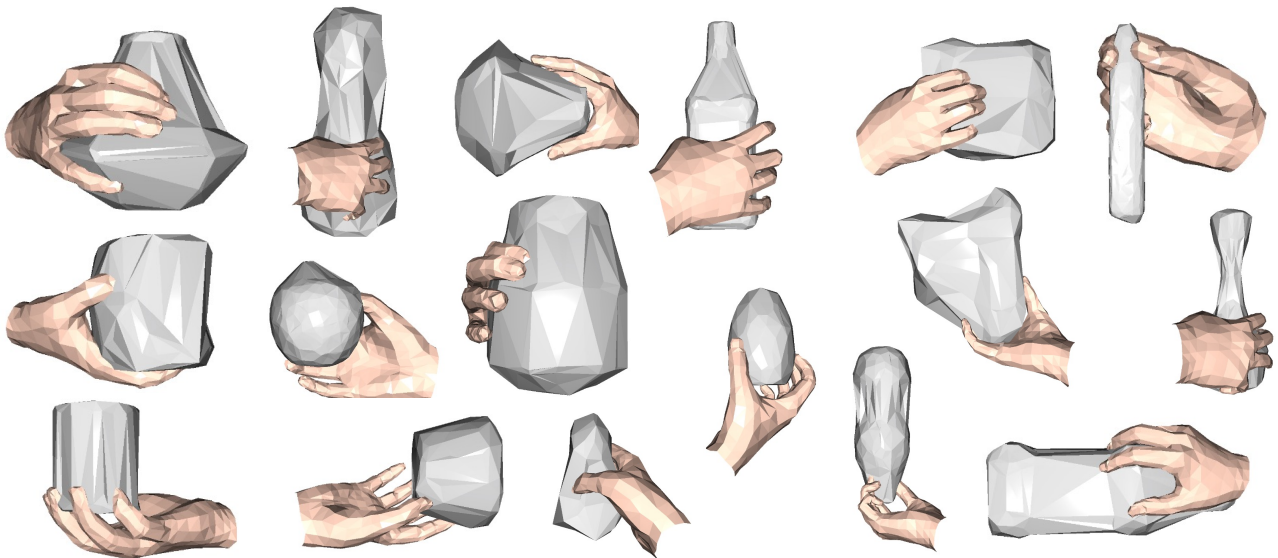


Figure 5. Samples of the unconditional generation of hand grasp together with objects.

Table 5. Statistics of the datasets used for training. ShapeNet contains the most object assets. However it is a generic object shape dataset, thus many included objects are not proper for hand grasp. OakInk-Shape contains rich grasp and object data but can not provide annotation for object transformation. We use the grasp data from GRAB and the object data from AffordPose as the supplement during training.

Datasets	#obj	#grasp	real/syn.	hand model
ShapeNet	51,300	-	real	-
GRAB [26]	51	1.3k	real	MANO [23]
OakInk-Image [33]	100	49k	real	MANO [23]
OakInk-Shape [33]	1,700	-	real + synthetic	MANO [23]
AffordPose [12]	641	26k	synthetic	GraspIt [16]
DexGraspNet [30]	5,355	1.32M	synthetic	ShadowHand [1]

erator can produce significantly fewer artifacts, especially artifact fingers, which have been a notorious issue in image generation recently. We provided some zoomed-in examples at the bottom. Moreover, compared to previous works using hand shapes to guide image generation [17, 35], we could generate both the object and the hand. Therefore, we could use the whole scene of hand-object interaction as the condition and thus enable more controllable details in the generated image.

E. Failure cases

To provide a transparent evaluation of our proposed method, we still notice some failure cases on the unseen objects from OakInk and GRAB datasets as shown in Figure 10. There are in general three patterns of failures: (1) the hand and the object have no contact, making the grasp physically implausible; (2) the hand skin is twisted or the pose is not able to grasp the object in human common sense; (3) the mesh of object and hand has penetration and intersection. There can be some reasons that make these happen. First of all, we do not explicitly supervise the contact between the object surface and hand as this is a rare annotation on many data sources, and calculating it can be computationally expensive. On the other hand, some implausible grasps have pretty good visual quality as shown in the middle two columns in the figure. However, according to our life experience, we know that the grasp is not physically plausible to manipulate the object. This has gone beyond our scope in this work as we do not have any physics-aware supervision such as the physical demonstration in a physics simulator. Finally, we use the object point cloud to represent object shapes to allow grasp generation on universal objects without a template, this causes the potential penetration between object mesh and hand mesh as the object mesh is ambiguous and unknown to our method. Despite the failure cases, we note that they make only a very small portion of the generated samples (less than 10% by a rough estimation). We show them here for transparency and to help discussion about future works in this area.



Figure 6. Given a single object, our method is capable of generating different grasps on it.



Figure 7. Samples of images generated by Adobe Firefly with synthesized hand grasp by our proposed method as the condition.



Figure 8. Using the same text-prompted image generation tool, we synthesize photo-realistic images with and without the grasp as the geometry condition. The grasp-conditioned image generation can have broad applications in image and video editing.

Not Grasp-conditioned

Grasp-conditioned



Holding a milk box



Holding a saki bottle



Receive a huge pencil



Holding a Whiskey flask



Holding a small vase



Hand over a vegetable



Figure 9. More examples of generating images of grasps with and without the condition from our generated grasps by the same image generation tool. Without a plausible grasp as the condition, there are more frequent unrealistic artifacts in the generated images, especially the number and pose of fingers. We provide some zoomed-in bad examples at the bottom.

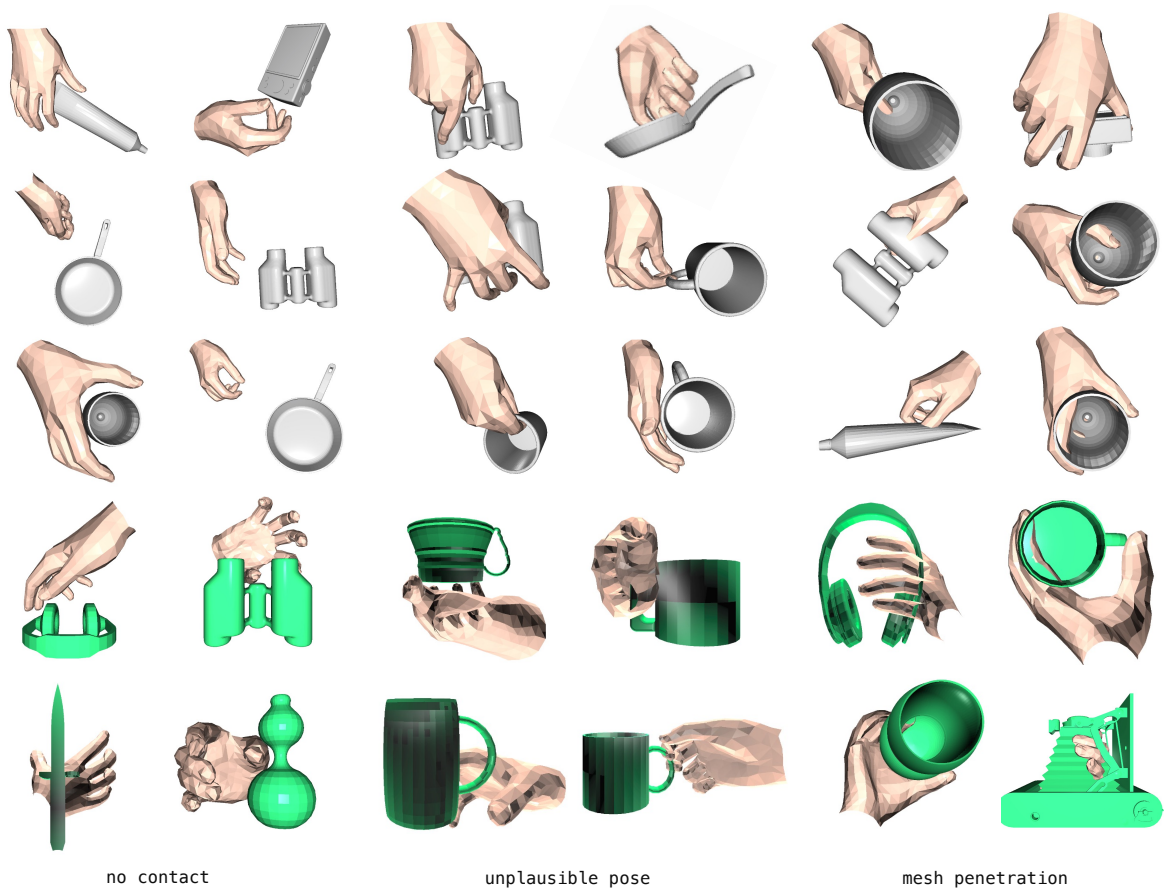


Figure 10. Bad samples of conditional grasp generation given objects from GRAB (gray) and OakInk-Shape (green).